Therapeutic Activity of DCC-2036, a Novel Tyrosine Kinase Inhibitor, against Triple-Negative Breast Cancer Patient-Derived Xenografts by Targeting AXL/MET

Yingying Shen[1*], Wei Zhang[2*], Jianghua Liu[1,3*], Jun He[4], Renxian Cao[1,3], Xiguang Chen[5], Xiuda Peng[1], Haifan Xu[6], Qiang Zhao[7], Jing Zhong[1], Wenjun Ding[1], Xiaoyong Lei[8], Yuyang Jiang[9] and Xuyu Zu[1]

[1]Institute of Clinical Medicine, The First Affiliated Hospital of University of South China, Hengyang, Hunan 421001, P.R. China. [2]Department of Biology, School of Medicine, Tsinghua University, Beijing 100084, P.R. China. [3]Department of Metabolism and Endocrinology, The First Affiliated Hospital of University of South China, Hengyang, Hunan 421001, P.R. China. [4]Department of Spine Surgery, The Affiliated Nanhua Hospital of University of South China, Hengyang, Hunan 421001, P.R. China. [5]Department of Medical Oncology, The First Affiliated Hospital of University of South China, Hengyang, Hunan 421001, P.R. China. [6]Department of Thyroid Breast Surgery, The First Affiliated Hospital of University of South China, Hengyang, Hunan 421001, P.R. China. [7]Department of Pathology, The First Affiliated Hospital of University of South China, Hengyang, Hunan 421001, P.R. China. [8]Institute of Pharmacy and Pharmacology, University of South China, Hengyang, Hunan 421001, P.R. China. [9]Guangdong Provincial Key Laboratory of Chemical Biology, Graduate School of Tsinghua University, Shenzhen 518055, P.R. China.

[*]Contributed equally

Correspondence: Professor Xuyu Zu, Institute of Clinical Medicine, The First Affiliated Hospital of University of South China, 69 Chuanshan Road, Hengyang, Hunan 421001, P.R. China. Tel: 86-734-8279382, Fax: 86-734-8279009; Professor Yuyang Jiang, Guangdong Provincial Key Laboratory of Chemical Biology, Graduate School at Shenzhen, Tsinghua University, Lishui Road, Shenzhen 518055, P.R. China. E-mail: zuxuyu0108@hotmail.com; jiangyy@sz.tsinghua.edu.cn

Accepted Article

Novelty and impact

The novel tyrosine kinase inhibitor DCC-2036 has potent activity against triple-negative breast cancer (TNBC) by targeting AXL/MET, especially AXL, and regulating the downstream PI3K/Akt-NFκβ pathway *in vitro* and *in vivo* (cell line and patient-derived xenograft models) without any obvious toxicity. Moreover, DCC-2036 exhibits more efficient antiproliferative activity in TNBC cells than most clinical drugs. These data strongly suggest DCC-2036 to be a promising targeting agent for treating TNBC, especially for tumors that overexpress AXL/MET.

Abstract

Triple-negative breast cancer (TNBC) is insensitive to endocrine therapy and targeted therapy to human epidermal growth factor receptor-2 (HER2), estrogen receptor (ER) and progesterone receptor (PR). New targets and new targeted therapeutic drugs for TNBC are desperately needed. The present study confirmed that DCC-2036 inhibited the proliferation, invasion, migration and epithelial-mesenchymal transition (EMT) of TNBC cells as well as induced apoptosis. Moreover, the antiproliferative activity of DCC-2036 was more efficient than that of most clinical drugs. In addition, the combination of DCC-2036 and cisplatin or lapatinib had synergistic effects on TNBC cells. Mechanistically, DCC-2036 targeted AXL/MET, especially AXL, and regulated the downstream PI3K/Akt-NF$\kappa\beta$ signaling to exert its antitumor effect in TNBC. DCC-2036 also inhibited the growth and metastasis of xenografted MDA-MB-231 cells (AXL/MET-high TNBC cells) but not MDA-MB-468 cells (AXL-low TNBC cells) in NSG mice *in vivo*. Furthermore, DCC-2036 significantly inhibited tumor growth and invasion of AXL/MET-high TNBC PDX tumors but not AXL/MET-low TNBC PDX tumors. These results highlighted the roles of AXL/MET in cancer growth and metastasis and further verified that the critical targets of DCC-2036 are AXL and MET, especially AXL. In addition, there was no significant toxicity of DCC-2036 even at a high dosage. Therefore, DCC-2036 may be a potential compound to treat TNBC, especially for tumors with AXL/MET overexpression.

Introduction

Triple-negative breast cancer (TNBC) accounts for 15-20% of all breast cancer cases and is phenotypically characterized by a lack of expression of estrogen receptor (ER), progesterone receptor (PR), and HER2 [1]. TNBC is related to advanced stage at diagnosis and worse outcome compared to other breast cancer subtypes [2]. TNBC is associated with a significantly shorter time to relapse [3]. Approximately 80% of TNBCs are classified as basal-like at the molecular level, and TNBC has significant overlap with the basal-like subtype [2].

In contrast to other subtypes of breast cancer, TNBC is not sensitive to hormonal therapies or treatments targeted against HER2. Chemotherapy is the sole systemic therapy for TNBC, but the prognosis remains poor [4, 5]. Research and development of targeted drugs against TNBC have attracted great attention in the past decade because targeted therapies have the advantage of maximizing efficacy while reducing toxicity [6, 7]. However, progress is still limited [8, 9], which is likely due to the molecular heterogeneity of TNBC and the lack of validated specific molecular targets [10, 11]. Therefore, novel targets and targeted agents for TNBC are urgently needed.

Recently, tyrosine kinases (TKs) have been suggested to be potential actionable targets due to their activation and high expression in multiple TNBC subtypes [12-15]. The success of Herceptin (trastuzumab) in HER2-positive breast cancer underlines the promise of targeting TKs. Nevertheless, tyrosine kinase inhibitors (TKIs) have had limited success in the clinic due to compensation signaling through alternative TK pathways [16-18]. Thus, to treat TNBC successfully, it will be necessary to inhibit multiple critical TKs and crucial signaling nodes downstream of oncogenic TK pathways.

DCC-2036, a third-generation TKI designed as a switch-control inhibitor of ABL1, shows remarkable efficacy in a murine bone marrow transplantation model of Bcr-Abl T315I chronic myeloid leukemia (CML) and potently suppresses T315I Bcr-Abl in primary patient cells [19, 20]. Our previous research also showed that DCC-2036 is also effective in imatinib-resistant cells expressing T674I FIP1L1-PDGFRα [21]. Moreover, DCC-2036 exhibits high selective activity for multiple TKs, including SRC, RAF,

VEGFR2, AXL and MET [20], which are activated and/or highly expressed in multiple TNBC subtypes [12, 22-24]. In the present study, the efficacy of DCC-2036 against TNBC was evaluated *in vitro* and *in vivo* (cell xenografts and patient-derived xenografts, PDXs), and the critical targets of DCC-2036 in TNBC were elucidated.

Materials and methods

Chemicals and antibodies

DCC-2036 (Rebastinib), cisplatin, paclitaxel, gemcitabine, doxorubicin and lapatinib were purchased from Selleck (Houston, TX, USA), and tamoxifen was purchased from Sigma-Aldrich (St. Louis, MO, USA). These compounds were dissolved in DMSO at a stock concentration of 20 or 40 mmol/L and stored at −20°C. The following immunoblotting antibodies were used: phospho-AXL (Y702) #5724, phospho-MET (Y1234/1235) #3077, MET #8198, β-actin #4970, phospho-AKT (S473) #4060, AKT #4691, phospho-IκBα #2859, IκBα #4812, phospho-P65 #3033, Lamin B1 #13435, E-cadherin #3195, Vimentin #5741, TCF-ZEB1 #3396, Snail #3879, Slug #9585 and Poly(ADP-ribose) polymerase (PARP) #9542, purchased from Cell Signaling Technology (Beverley, MA, USA); AXL #20741, purchased from Santa Cruz (Santa Cruz, CA, USA); P65 #16502, purchased from Abcam (Cambridge, MA, USA); GAS6 #13795-1-AP, HGF #26881-1-AP, AXL #13196-1-AP, purchased from Proteintech (Wuhan, Hubei, china); and horseradish peroxidase (HRP)-conjugated secondary antibodies #AP-132P, purchased from Merck Millipore (Darmstadt, Germany).

Cell culture

The basal-like/TNBC cell lines MDA-MB-231 and HS-578T and the luminal breast cancer cell lines MCF-7 and T47D were purchased from American Type Culture Collection (ATCC, Manassas, VA, USA). The MDA-MB-436 and MDA-MB-468 basal-like/TNBC cell lines, the ZR-75-1 luminal breast cancer cell line and the SK-BR-3 HER2-positive breast cancer cell line were obtained from the Cell Bank at the Chinese Academy of Sciences (Shanghai, China). All cells were cultured in

DMEM (Gibco, Waltham, MA, USA) supplemented with 10% heat-activated fetal bovine serum (Biological Industries, Northern Kibbutz Beit Haemek, Israel) and 1% penicillin/streptomycin at 37˚C with 5% CO_2. The cell lines were characterized by the Genetic Testing Biotechnology Corporation (Suzhou, Jiangsu, China) using short tandem repeat (STR) markers.

Cell viability assay

Cell viability was evaluated by an MTS assay (CellTiter 96 Aqueous One Solution Cell Proliferation assay; Promega, Madison, WI, USA) [25]. Cells (3×10^3/well) plated in 96-well plates were treated with various concentrations of DCC-2036 or other drugs (cisplatin, paclitaxel, gemcitabine, doxorubicin, lapatinib or tamoxifen) for 72 h. The absorbance/optical density was measured with a 96-well plate reader at a wavelength of 490 nm after the addition of MTS solution. The drug concentration resulting in 50% inhibition of cell growth (IC_{50}) was determined. Combination index (CI) studies with MDA-MB-231 cells were performed as previously described [26].

Colony-formation assay

MDA-MB-231 and HS-578T cells (2×10^5/well) plated in 6-well plates were treated with 0 or 3.75 μM DCC-2036 for 48 h; then, the cells were collected, washed with PBS and cultured in DMEM lacking drugs. Fourteen days later, the cells were washed with PBS, fixed in 10% methanol for 15 min, and stained with Giemsa for 20 min. Colonies that consisted of >50 cells were counted under an inverted microscope. The colony-formation ability was assessed.

Flow cytometry

Measurement of apoptosis and analysis of cell cycle were performed as previously described [21, 27].

Transwell cell invasion and migration assay

The transwell cell invasion and migration assays were performed as previously

described [28]. Invasive and migrated cells adhering to the undersurface of the filter were counted (five fields per chamber) using an inverted microscope (10×). The migration assay was performed similarly to the invasion assay, except that Matrigel was used only for the invasion assay, and the permeating time for cells differed (migration, 24 h; invasion, 48 h).

Antibody array and global cDNA microarray

For antibody array analysis, the PathScan RTK Signaling Antibody Array Kit (Cell Signaling Technology) was used following the manufacturer's protocol. Quantification of the different RTKs in the human phospho-RTK array kit was performed using ImageJ 1.44 software (National Institute of Health) [29]. The global cDNA microarray analysis was performed as previously described [30]. The data were deposited in the NCBI Gene Expression Omnibus (Edgar *et al*., 2002) and are accessible through GEO Series accession number GSE109230 (https://www.ncbi.nlm.nih.gov/geo/query/acc.cgi?acc=GSE109230).

Real-time RT-PCR

Total RNA was extracted from cells using TRIzol reagent (Invitrogen; Thermo Fisher Scientific, Waltham, MA, USA). Isolated RNA was reverse transcribed using the RevertAid First Strand cDNA Synthesis Kit (Thermo Fisher Scientific) according to the manufacturer's protocol. The following primers were used: AXL forward, 5'-GACATAGGGCTAAGGCAAGAGG-3'; AXL reverse, 5'-CGAGAAGGCAGGAGTTGAAGG-3'; MET forward, 5'-TGCAGCGCGTTGACTTATTCATGG-3'; MET reverse, 5'-GAAACCACAACCTGCATGAAGCGA-3'; GAPDH forward, 5'-TGACTTCAACAGCGACACCCA-3'; and GAPDH reverse, 5'-CACCCTGTTGCTGTAGCCAAA-3'. Quantitative measurement of target gene mRNA levels was performed using the ABI Prism 7500 Sequence Detection System (Applied Biosystems; Thermo Fisher Scientific). The data were analyzed using the $2^{-\Delta\Delta Cq}$ method [31].

Western blotting analysis

Whole lysates were prepared with radioimmunoprecipitation assay (RIPA) buffer as described previously [30]. The cytosolic and nuclear fractions were prepared with a Nuclear Extraction Kit (Merck Millipore) according to the manufacturer's protocol.

Transfection

AXL and MET plasmids were purchased from Genechem (Shanghai, China) and transfected into cells using Lipofectamine 2000 (Invitrogen; Thermo Fisher Scientific) according to the manufacturer's protocol. Twenty-four hours after transfection, cells were exposed to 5 μM DCC-2036 for 48 h. Cell death and related protein levels were detected. The AXL siRNA (5'-GCCUGACGAAAUCCUCUAUTT-3'), MET siRNA (5'-CTCATTTGGATAGGCTTGTAA-3') and negative control siRNA (5'-UUCUCCGAACGUGUCACGUTT-3') were obtained from GenePharma (Shanghai, China). siRNAs were transfected into cells using Lipofectamine RNAiMAX (Invitrogen; Thermo Fisher Scientific) according to the manufacturer's protocol.

NOD-SCID IL-2 receptor gamma null (NSG) mouse xenograft model

Fourteen female NSG mice were obtained from IDMO Co., Ltd (Beijing, China). The mice were housed in barrier facilities with a 12-h light dark cycle, with food and water available *ad libitum*. MDA-MB-231 cells (5×10^6) resuspended in 200 μL of Matrigel (Becton Dickson, Mississauga, ON, Canada) were inoculated subcutaneously in the right flanks of 4-week-old female NSG mice. The tumors were measured twice a week with calipers. Tumor volumes were calculated with the following formula: $a^2 \times b \times 0.5$; where *a* is the smallest diameter, and *b* is the diameter perpendicular to a. DCC-2036 (100 mg/kg/d) was dissolved in 0.5% carboxymethylcellulose (CMC)/1% Tween 80 (Sigma-Aldrich). The mice in the control group received 0.5% CMC/1% Tween 80. The body weight, feeding behavior and motor activity of each animal were monitored as indicators of general health. The

animals were then euthanized, and the tumor xenografts were immediately removed, weighed, stored and fixed. This study was conducted based on the recommendations in the Guide for the Care and Use of Laboratory Animals of the National Institutes of Health. Sodium pentobarbital anesthesia methods and other efforts were taken to minimize animal suffering. Immunohistochemical staining (Ki-67) and H&E staining were performed as previously described [27]. The MDA-MB-468 cell line xenograft model was performed the same as the MDA-MB-231 cell line xenograft model.

Patient-derived xenograft (PDX) models. IDMO-129 and 862812 patient-derived TNBC xenografts were derived at Beijing IDMO Co., Ltd. and our institute, and the studies were performed at Beijing IDMO Co., Ltd. Primary grafts (P0) and low-passage PDXs (≤P5) were used for all therapeutic experiments. Tumors were transplanted in the subcutaneous tissue of 6- to 8-week-old female NSG mice and treated with 150 mg/kg DCC-2036 or solvent (0.5% CMC/1% Tween 80) once daily when the tumor volume reached an average volume of 120 mm^3. The subsequent experiments were performed as described above. The AXL antibody (R&D, Lille, France, #AF154, 1:100) and MET antibody (Cell Signaling Technology, #8198, 1:50) were used for immunohistochemical staining. In the combination models, 100 mg/kg DCC-2306 was administered three times a week, and 6 mg/kg cisplatin was administered once a week. Percent tumor growth inhibition (TGI) was determined by the following formula: $\%TGI=[(C_t-C_0)-(T_t-T_0)]/(C_t-C_0)\times100$; where T_t is the treated tumor volume at time t; T_0 is the treated tumor volume at the start of dosing; C_t is the control tumor volume at time t; and C_0 is the control tumor volume at the start of dosing [32].

Statistical analysis

All experiments were performed at least three times, and the results are expressed as the mean±standard deviation (SD) unless otherwise stated. GraphPad Prism 5.0 software (GraphPad Software) was used for statistical analysis. Comparisons between two groups involved two-tailed Student's *t* test, and comparisons among multiple

groups involved one-way ANOVA with *post hoc* intergroup comparison using Tukey's test. A P value of <0.05 was considered significant.

Results

DCC-2036 significantly inhibits human TNBC cell proliferation

The effect of DCC-2036 was first analyzed on the growth of MDA-MB-231 and HS-578T (TNBC cells), and other commonly used drugs for breast cancer were also analyzed for comparison. Cells were treated with increasing concentrations of DCC-2036 or other chemotherapeutics for 72 h, and cell viability was then measured using the MTS assay. DCC-2036 inhibited the growth of MDA-MB-231 and HS-578T cells with an inhibitory concentration (IC_{50}) of 3.3 μM and 3.7 μM, respectively (Fig. 1A), which was more efficient than cisplatin, gemcitabine, lapatinib, tamoxifen, 5-FU and gefitinib [33] (Table 1, Supplementary Fig. S1A). In addition, the combination of DCC-2036 and cisplatin or lapatinib had a synergistic effect (Supplementary Fig. S1B). Furthermore, the effect of DCC-2036 on the growth of the MCF-7 cell line, which is a luminal breast cancer cell line (ER+PR+HER2-), was also analyzed. Unexpectedly, the IC_{50} of MCF-7 cells was 9.0 μM (Fig. 1A), indicating that TNBC cells were more sensitive than luminal cells to DCC-2036.

Because clonogenicity is a better indicator of the ability of long-term proliferation in malignant tumor cells, this characteristic was evaluated in MDA-MB-231 and HS-578T cells. Both cell lines were exposed to various concentrations of DCC-2036 for 48 h and then plated in DMEM lacking DCC-2036. DCC-2036 significantly inhibited the surviving clonogenic fraction of TNBC cells (Fig. 1B).

To investigate whether DCC-2036 affected the cell cycle distribution, MDA-MB-231 and HS-578T cells were treated with 3.75 μM DCC-2036 for 48 h, and their DNA content was analyzed using flow cytometry. G1 arrest was induced by DCC-2036 in TNBC cells (Fig. 1C).

DCC-2036 induces apoptosis and inhibits TNBC cell migration and invasion

The proapoptotic effect of DCC-2036 was confirmed by flow cytometry after dual staining of AnnexinV-FITC/PI. DCC-2036 induced apoptosis in MDA-MB-231, HS-578T and MCF-7 cells in a dose-dependent manner, but DCC-2036 had a higher

apoptosis induction effect in the TNBC cell lines than in the luminal cell line. The cell death rate of MCF-7 cells treated with 5 μM and 10 μM DCC-2036 was approximately 36% and 47%, respectively, while the cell death rate of MDA-MB-231 cells and HS-578T cells treated with 5 μM DCC-2036 was approximately 52% and 67%, respectively (Fig. 2A).

The migration and invasion of MDA-MB-231 and HS-578T cells were examined after DCC-2036 treatment. Treatment with 3.75 μM DCC-2036 for 48 h resulted in an approximately 3- to 4-fold reduction in migration and invasion of MDA-MB-231 cells. Consistently, treatment with 3.75 μM DCC-2036 for 48 h led to a 2- to 3-fold reduction in the migration and invasion of HS-578T cells (Fig. 2B).

Identification of the critical therapeutic targets of DCC-2036 in TNBC

For DCC-2036 is a multitarget TKI, the activity change of TKs was explored by analyzing the tyrosine phosphorylation of receptor tyrosine kinases (RTKs) and the phosphorylation of specific activating residues in signaling proteins. The activation status of 28 RTKs and 11 important signaling nodes was analyzed in MDA-MB-231 cells cultured with or without DCC-2036 using antibody arrays. DCC-2036 treatment downregulated 21 RTKs, including MET/HGFR, TrkB/NTRK2, FGFR4, VEGFR2/KDR and AXL, as well as 6 important signaling nodes, including Akt/PKB/Rac (Thr308), Akt/PKB/Rac (Ser473), p44/42 MAPK (ERK1/2), S6 Ribosomal Protein (Ser235/236), c-Abl and Src (Fig. S2A).

To better understand the molecular mechanisms involved in the effect of DCC-2036 on TNBC cells, the whole genome-wide transcriptome profile of MDA-MB-231 cells cultured with or without DCC-2036 was analyzed by cDNA microarray. According to fold-change (2.0×) screening between the control and drug-treatment groups, a total of 4659 genes had altered expression, of which 2034 and 2625 were upregulated and downregulated, respectively. Most of these differentially expressed genes were involved in the cell cycle, signal transduction and carcinogenesis (Fig. S3). Twelve TK genes were downregulated and were selected for cluster mapping on the MeV microarray analysis platform (Fig. S2B). Furthermore, only AXL and MET were

reduced significantly in both activity and expression as observed when comparing the results of Fig. S2A and S2B. Based on the kinase inhibition profile of DCC-2036 (AXL IC_{50}=42 nM; MET IC_{50}=250 nM) [20], AXL and MET may be the key targets of DCC-2036 in TNBC.

To demonstrate that the critical targets of DCC-2036 are AXL/MET, eight different breast cell lines were used to assess the levels and activity of AXL and MET as well as the presence of their ligands by blotting (Fig. S4A). The sensitivities of different cells to DCC-2036 were determined by MTS assay (Fig. 1A and Fig. S4B). The sensitivity of TNBC cell lines to DCC-2036 positively correlated with the activity, total level and ligands of AXL and MET, especially AXL, which is overexpressed in most TNBC cell lines. MDA-MB-436 cells with moderate AXL expression were sensitive to DCC-2036 but showed inferior sensitivity to MDA-MB-231 and HS-578T cells with high AXL expression. MDA-MB-468 cells showed resistance to DCC-2036 due to the absence of AXL. In non-TNBC cell lines, the deficiency of AXL is ubiquitous. Thus, TNBC cells lines showed higher sensitivity to DCC-2036 than non-TNBC cell lines. Notably, non-TNBC cell lines were not resistant to DCC-2036 but were relatively insensitive, which indicated the existence of other DCC-2036 targets in non-TNBC cells. These findings indicated that the critical therapeutic targets of DCC-2036 in TNBC are AXL and MET, especially AXL.

DCC-2036 inhibits the PI3K/Akt-NFκβ pathway and epithelial-mesenchymal transition (EMT) by targeting AXL/MET in TNBC cells

The mRNA levels of AXL and MET were downregulated in MDA-MB-231 cells treated with DCC-2306 according to real-time PCR (Fig. 3A), which was consistent with the cDNA microarray. Western blot analysis showed that the phosphorylation level and protein content of AXL and MET were both downregulated, and the phosphorylation level decreased more rapidly after DCC-2036 treatment in MDA-MB-231 and HS-578T cells. Interestingly, the phosphorylation level and the total amount of AXL were both increased by DCC-2036 treatment in MCF-7 cells (Fig. 3B), which further explained why luminal cells were less sensitive to DCC-2036

than TNBC cells. To further confirm a more detailed target of DCC-2036 in TNBC cells, the impact of AXL or MET on the sensitivity of MDA-MB-231 cells to DCC-2036 was evaluated. Transfection of the AXL plasmid into MDA-MB-231 cells induced sufficient upregulation of AXL as measured by Western blot analysis (Fig. 3C, top). AXL overexpression remarkably attenuated DCC-2036-induced apoptosis compared with the vector control as analyzed by immunoblotting for PARP cleavage (Fig. 3C, top) and trypan blue exclusion assay (Fig. 3C, bottom). Similar results were found with MET overexpression but to a lower extent than AXL. In addition, AXL or MET was knocked down in MDA-MB-231 cells, and the effects of DCC-2036 were analyzed by MTS assay and flow cytometry. As shown in Fig. S5B, AXL or MET knockdown inhibited MDA-MB-231 cell proliferation, especially AXL knockdown. AXL or MET knockdown partly reversed the DCC-2036-induced proliferation inhibition and cell death in MDA-MB-231 cells, especially AXL knockdown (Fig. S5C and D). Therefore, these data suggested that AXL is the most critical target of DCC-2036 in TNBC.

To elucidate the mechanism involved in the effect of DCC-2036 on TNBC cells, the NFκβ pathway was investigated because this pathway acts downstream of the PI3K/Akt pathway, is a downstream target of AXL/MET activation and is involved in the regulation of cell proliferation, apoptosis and EMT [34, 35]. Therefore, PI3K/Akt-NFκβ pathway-related protein expression with or without DCC-2036 treatment was examined in MDA-MB-231 and HS-578T cells. P-Akt, P-IκBα, P-P65 and P65 were downregulated, and IκBα was upregulated, revealing the downregulation of the PI3K/Akt-NFκβ pathway by DCC-2036 (Fig. 3D). Moreover, a nuclear separation experiment demonstrated that DCC-2036 inhibited the degradation of IκBα and the nuclear translocation of p65 in MDA-MB-231 cells (Fig. 3E).

Cell migration and invasion could be driven by EMT [36]. To determine whether DCC-2036 has a role in EMT induction, the effect of DCC-2036 on the expression of EMT markers was assessed. DCC-2036 strongly upregulated E-cadherin expression, while the expression of mesenchymal markers, such as Vimentin, TCF-ZEB1, Snail and Slug, was downregulated in MDA-MB-231 and HS-578T cells (Fig. 3F).

DCC-2036 inhibits the growth and metastasis of xenografted MDA-MB-231 cells in NSG mice

The *in vivo* effect of DCC-2036 on MDA-MB-231 cells (AXL/MET-high TNBC cells) was further evaluated using the NSG mouse xenograft model. MDA-MB-231 cells were inoculated subcutaneously in 14 NSG mice. When the tumor size reached approximately 150 mm^3, the mice were randomized to receive treatment with 0.5% carboxymethylcellulose/1% Tween 80 (Control) or DCC-2036 (100 mg/kg/d, oral gavage administration) for 22 days. This DCC-2036 dosage was well tolerated because the body weights of the mice were stable with no obvious distinctions between treated and control mice (Fig. 4B). Motor activity and feeding behavior were normal (data not shown). Inspection of morbidity and mortality did not reflect significant toxicity of DCC-2036 at the dosage used. Based on the growth curve, DCC-2036 attenuated the growth of MDA-MB-231 tumors (Fig. 4A). DCC-2036-treated tumors were smaller and weighed less than control tumors (Fig. 4C). Compared with the control group (lung metastasis incidence: 3/7, 42.9%), mice that received DCC-2036 treatment showed a 26.2% reduction in the incidence of lung metastasis (1/6, 16.7%) (Fig. 4D). Immunohistochemical analysis with an anti-Ki67 antibody (to detect cell proliferation status) implied that Ki67 immunoreactivity was inhibited by DCC-2036 treatment, which indicated that cell proliferation was inhibited by DCC-2036 (Fig. 4E). Immunoblotting of xenograft tissues from mice demonstrated that DCC-2036 potently inhibited AXL/MET, the downstream PI3K/Akt-NFκβ pathway, and EMT, which was consistent with the *in vitro* data (Fig. 4F). At the same dosage, however, DCC-2036 did not inhibit the growth and metastasis of xenografted MDA-MB-468 cells (AXL-low TNBC cells) in NSG mice (Fig. S6). Thus, these data revealed the *in vivo* antitumor activity of DCC-2036 against human TNBC cells with high AXL/MET expression, and these findings suggested that AXL level may be used to predict DCC-2036 sensitivity in TNBC.

DCC-2036 inhibits patient-derived xenograft growth

With the aim of using a more relevant preclinical model, two TNBC PDXs generated at IDMOTech and our institute were evaluated. Table S1 shows the relevant information for these two patients. Fresh TNBCs from the two patients, IDMO-129 and 862812, were grafted directly into the subcutaneous tissue of NSG mice (Fig. S7A). The PDXs histologically resembled the parental TNBCs, and they had similar ER, PR, HER2 and Ki67 expression (Fig. S7B). Real-time PCR analysis showed that AXL and MET mRNA were highly expressed in IDMO-129 PDX but lowly expressed in 862812 PDX. As assessed by Western blot, AXL and MET protein expression levels (including the phosphorylated and total protein levels) correlated with mRNA levels (Fig. 5A). Moreover, IDMO-129 PDX, which had higher AXL and MET levels, also showed a faster growth rate than the 862812 PDX (Fig. 5B).

The effect of DCC-2036 on the growth of AXL/MET-high IDMO-129 and AXL/MET-low 862812 PDXs was investigated. At the end of treatment, IDMO-129 growth was significantly reduced (by 57.4%) in DCC-2036-treated mice compared with the untreated group (solvent) (P<0.05) (Fig. 5B, left and Fig. S8, left). However, growth of the AXL-low 862812 PDX was reduced (by 38.8%) with DCC-2036 treatment, but the difference was not significant (Fig. 5B, right and Fig. S8, right). Moreover, the DCC-2036 dosage (150 mg/kg/d) was well tolerated since there was a less than 20% change in body weight between treated and control mice in these two PDXs (Fig. 5C), indicating that there was no significant toxicity of DCC-2036 even at the high dosage. DCC-2036-treated tumors were smaller and weighed less than control tumors in IDMA-129 PDX (Fig. 5D), but there was no obvious difference in 862812 PDX (Fig. 5E). Immunohistochemical analysis implied that AXL, MET and Ki67 immunoreactivity was remarkably inhibited by DCC-2036 treatment in IDMA-129 PDX (Fig. 5F). In contrast, these markers were not significantly affected by DCC-2036 in 862812 PDX (Fig. S9A). Immunoblotting of xenograft tissues from IDMO-129 PDX showed that DCC-2036 potently inhibited AXL/MET, the downstream PI3K/Akt-NFκβ pathway and EMT (Fig. 5G). However, DCC-2036 exhibited a minimal inhibitory effect of these critical signaling nodes in 862812 PDX

(Fig. S9B). In addition, IDMO-129 PDX was used to evaluate the combination effect of DCC-2306 and cisplatin *in vivo*. The combination of DCC-2306 and cisplatin was more efficient than DCC-2036 or cisplatin alone (Fig. S10A). However, note that the body weights in the DCC-2036 group were stable, but the body weights in the cisplatin and combination groups decreased (Fig. S10B), reflecting the safety of DCC-2036 and the toxicity of cisplatin.

Discussion

Breast cancer is heterogeneous with major subtypes defined by expression of ER, PR and HER2. Approximately 70% of breast cancers are luminal subtype (ER- and/or PR-positive), and these tumors are sensitive to hormonal therapies, such as tamoxifen. Another subset of breast cancer is characterized by HER2 overexpression, and these tumors are often typically responsive to HER2-directed agents, such as trastuzumab. Nevertheless, approximately 15–20% of breast cancers are classified as TNBC, which lack expression of these three molecules, hence precluding the use of endocrine or anti-HER2 targeted therapies. Moreover, TNBC is the most aggressive subtype of breast cancer with frequent and rapid relapse [37]. Chemotherapy is the only systemic therapy available for TNBC. Currently, the use of targeted therapies in breast cancers is increasing, especially when conventional chemotherapy affords relatively small benefits at a cost of increased toxicity. TKIs may be a good choice because TKs are often activated and highly expressed in multiple TNBC subtypes and might be potential targets [15, 38]. However, most TKIs show limited efficacy against TNBC, although some have entered clinical trials. For instance, dasatinib (a SRC family kinase inhibitor) and sorafenib (a VEGFR/Raf inhibitor) displayed moderate efficacy in TNBC patients when utilized as a single agent [39, 40]. Unexpectedly, the combination of dasatinib and sorafenib exhibited an enhanced efficacy compared with the single use of either dasatinib or sorafenib in inhibiting TNBC [41], indicating an advantage using agents concurrently to target multitargets in the treatment of TNBC. As a novel third-generation TKI, DCC-2036 has a broader kinase inhibition profile than second-generation TKIs, such as dasatinib, sorafenib and gefitinib. DCC-2036

potently inhibits multitargets, including SRC, RAF, VEGFR2, AXL and MET [20], which are activated and/or highly expressed in multiple TNBC subtypes [12, 22-24]. The present study indicated that DCC-2036 efficiently inhibits TNBC *in vitro* and *in vivo*. First, DCC-2036 showed more potent antiproliferative activity in TNBC cell lines (MDA-MB-231 and HS-578T) than most common clinically used drugs for breast cancer, including cisplatin, gemcitabine, lapatinib, tamoxifen, 5-FU and gefitinib. DCC-2036 also significantly inhibited the colony-forming capability and induced G1 arrest in TNBC cells. Second, DCC-2036 induced apoptosis, inhibited EMT and inhibited migration/invasion of TNBC cell lines. Third, DCC-2036 exhibited considerable antitumor activity at the indicated dose in the MDA-MB-231 xenograft NSG model. DCC-2036 inhibited not only growth but also the metastasis of xenografted MDA-MB-231 cells in NSG mice. The xenograft NSG model was selected instead of the nude mouse model since the NSG model is internationally recognized as the highest immunodeficiency and is therefore the most suitable mouse model for human cell transplantation. In addition, the TNBC PDX model, IDMO-129, was also inhibited by DCC-2036 with no obvious toxicity.

The mechanism investigation indicated that the effect of DCC-2036 on TNBC occurred mainly through the suppression of AXL/MET-PI3K/Akt-NFκβ signaling. AXL, a member of the TAM (TYRO3, AXL and MER) RTK family, is hyperactivated and overexpressed in a majority of the most aggressive TNBC cell lines [12]. Furthermore, following binding to its ligand, growth arrest specific 6 (GAS6), AXL dimerizes and consequently activates various intracellular pathways, which regulate many biological processes, such as cell apoptosis, proliferation, migration, invasion, angiogenesis and drug resistance [23, 42]. MET, also named hepatocyte growth factor receptor (HGFR), is an RTK highly expressed in TNBC [43], and MET expression correlates with poor prognosis [15]. The AXL and MET kinases share a number of structural features and similarly play important roles in tumor formation, development and drug resistance [42]. The present study confirmed these two RTKs as the critical and suitable targets of DCC-2036 in TNBC for the following reasons: 1) Although certain other RTKs, such as FLT3, Ron, and Ret, exhibited larger fold changes than AXL or

MET in the RTK antibody arrays, they did not show high expression in TNBC cells and low expression in luminal cells as shown with AXL and MET, which could serve as therapeutic targets for TNBC. 2) Western blot analysis showed that the phosphorylation level and total protein content of AXL and MET were both downregulated after DCC-2036 treatment. However, the phosphorylation level of AXL and MET decreased more rapidly, which suggested that the decrease in p-AXL and p-MET was not completely due to the downregulation of T-AXL and T-MET. 3) RTKs can be a inducer of EMT progression, and can also be regulated by different EMT transcription factors [44, 45]. AXL is an EMT-induced regulator of cancer metastasis under the control of Slug and Vimentin in breast cancer [46-49]. Thus, the total levels of AXL/MET may be downregulated by EMT transcription factors, such as Slug, or other transcription factors that should be further investigated. In addition, the FRA-1 transcription factor is downstream of AXL and upstream of MET [49], suggesting that MET might also be regulated by AXL. 4) The IC50 values of AXL and MET (42 nM and 250 nM, respectively, according to *in vitro* kinase assays) are less than other kinases. The IC50 value of Ron is 300 nM, and DCC-2036 has not been reported to inhibit Ret or ROR1 [20]. Thus, they are not considered to direct targets of DCC-2036. 5) Ectopic expression of AXL and MET attenuated DCC-2036-induced apoptosis in TNBC cells. 6) Treatment with DCC-2036 significantly inhibited tumor growth and invasion in AXL/MET-high TNBC PDX but not in AXL/MET-low TNBC PDX. In summary, AXL and MET are at least two of the most critical targets of DCC-2036 in TNBC rather than transcriptional targets of other RTKs targeted by DCC-2036. To further establish which RTK (AXL or MET) is the most important target of DCC-2036, the effects of DCC-2036 were analyzed in cell lines specifically depleted for AXL or MET. Moreover, a wider panel of breast cancer cell lines was used, in which the levels and activity of both AXL and MET as well as the presence of their ligands and their correlation with DCC-2036 sensitivity were analyzed. These experiments supported that AXL is the most critical target of DCC-2036 in TNBC. Although TNBC cell lines are commonly AXL positive, AXL expression in patients is not limited to this breast cancer subtype [50]. Thus, it would be interesting to extend the

therapeutic use of DCC-2036 to other breast cancer subtypes with high AXL expression. To confirm the notion that AXL level rather than TNBC subtype could be used to predict DCC-2036 sensitivity, MDA-MB-468 cells were transplanted into NSG mice because this TNBC cell line lacks AXL expression. MDA-MB-468 cells were resistant to DCC-2036 i*n vitro*, and the same phenomenon was observed *in vivo*. These results indicated that AXL level may be used to predict DCC-2036 sensitivity in TNBC.

EGFR is often overexpressed in TNBC cells, thus making TNBC more difficult to treat and notably lowering the 10-year survival rate in breast cancer patients [51]. EGFR, AXL and MET receptors can coexist in local clusters on the plasma membrane, leading to subsequent activation-dependent enhancement of interactions after stimulation. A switch from an EGFR pathway-dependent signal transduction pattern to an AXL/MET complex-dependent pattern plays critical roles in acquired EGFR TKI, such as lapatinib and erlotinib resistance-correlated EMT [42]. Therefore, DCC-2036 may be efficacious in counteracting such signal diversification and overcoming EGFR TKI resistance by disrupting this complex interaction. In addition, AXL is relevant to resistance to chemotherapy, such as cisplatin [52-54]. Hence, a combination of DCC-2036 with chemotherapy or other TKIs may be a novel therapeutic approach in TNBC. Indeed, the present results showed that the combination of DCC-2036 and cisplatin or lapatinib had synergistic effects on TNBC. Moreover, cisplatin at the normal dosage [55] had a substantially greater toxicity than DCC-2306 at a high dosage *in vivo*.

Downstream activation of the PI3K/Akt-NFκB pathway can persist in the presence of MET/AXL coexpression [34, 35, 42]. Therefore, PI3K/Akt-NFκβ pathway-related protein expression was examined in TNBC cells with or without DCC-2036 treatment. As expected, the PI3K/Akt-NFκβ pathway was inhibited by DCC-2036 *in vitro* and *in vivo*.

In summary, these data demonstrated that DCC-2036 has potent activity against TNBC cells by targeting AXL/MET, especially AXL, *in vivo* and *in vitro* without any obvious toxicity. DCC-2036 exhibits more efficient antiproliferative activity in TNBC

cells than most common clinically used drugs, suggesting that DCC-2036 is a promising targeting agent for treating TNBC with AXL/MET overexpression or other tumors driven by AXL/MET.

References

1. Metzger-Filho O, Tutt A, de Azambuja E, Saini KS, Viale G, Loi S, Bradbury I, Bliss JM, Azim HA, Jr., Ellis P, Di Leo A, Baselga J, et al. Dissecting the heterogeneity of triple-negative breast cancer. *J Clin Oncol* 2012;**30**: 1879-87.

2. Foulkes WD, Smith IE, Reis-Filho JS. Triple-negative breast cancer. *N Engl J Med* 2010;**363**: 1938-48.

3. Dent R, Trudeau M, Pritchard KI, Hanna WM, Kahn HK, Sawka CA, Lickley LA, Rawlinson E, Sun P, Narod SA. Triple-negative breast cancer: clinical features and patterns of recurrence. *Clin Cancer Res* 2007;**13**: 4429-34.

4. Gluz O, Liedtke C, Gottschalk N, Pusztai L, Nitz U, Harbeck N. Triple-negative breast cancer--current status and future directions. *Ann Oncol* 2009;**20**: 1913-27.

5. Xu L, Yin S, Banerjee S, Sarkar F, Reddy KB. Enhanced anticancer effect of the combination of cisplatin and TRAIL in triple-negative breast tumor cells. *Mol Cancer Ther* 2011;**10**: 550-7.

6. Lin NU, Claus E, Sohl J, Razzak AR, Arnaout A, Winer EP. Sites of distant recurrence and clinical outcomes in patients with metastatic triple-negative breast cancer: high incidence of central nervous system metastases. *Cancer* 2008;**113**: 2638-45.

7. Anders CK, Winer EP, Ford JM, Dent R, Silver DP, Sledge GW, Carey LA. Poly(ADP-Ribose) polymerase inhibition: "targeted" therapy for triple-negative breast cancer. *Clin Cancer Res* 2010;**16**: 4702-10.

8. Carey L, Winer E, Viale G, Cameron D, Gianni L. Triple-negative breast cancer: disease entity or title of convenience? *Nat Rev Clin Oncol* 2010;**7**: 683-92.

9. Hudis CA, Gianni L. Triple-negative breast cancer: an unmet medical need. *Oncologist* 2011;**16 Suppl 1**: 1-11.

10. Lehmann BD, Bauer JA, Chen X, Sanders ME, Chakravarthy AB, Shyr Y, Pietenpol JA. Identification of human triple-negative breast cancer subtypes and preclinical models for selection of targeted therapies. *J Clin Invest* 2011;**121**: 2750-67.

11. Burstein MD, Tsimelzon A, Poage GM, Covington KR, Contreras A, Fuqua SA, Savage MI, Osborne CK, Hilsenbeck SG, Chang JC, Mills GB, Lau CC, et al. Comprehensive genomic analysis identifies novel subtypes and targets of triple-negative breast cancer. *Clin Cancer Res* 2015;**21**: 1688-98.

12. Wu X, Zahari MS, Ma B, Liu R, Renuse S, Sahasrabuddhe NA, Chen L, Chaerkady R, Kim MS, Zhong J, Jelinek C, Barbhuiya MA, et al. Global phosphotyrosine survey in triple-negative breast cancer reveals activation of multiple tyrosine kinase signaling pathways. *Oncotarget* 2015;**6**: 29143-60.

13. Jiao Q, Wu A, Shao G, Peng H, Wang M, Ji S, Liu P, Zhang J. The latest progress in research on triple negative breast cancer (TNBC): risk factors, possible therapeutic targets and prognostic markers. *J Thorac Dis* 2014;**6**: 1329-35.

14. Craig DW, O'Shaughnessy JA, Kiefer JA, Aldrich J, Sinari S, Moses TM, Wong S, Dinh J, Christoforides A, Blum JL, Aitelli CL, Osborne CR, et al. Genome and transcriptome sequencing in prospective metastatic triple-negative breast cancer uncovers therapeutic vulnerabilities. *Mol Cancer Ther* 2013;**12**: 104-16.

15. Fleisher B, Clarke C, Ait-Oudhia S. Current advances in biomarkers for targeted therapy in triple-negative breast cancer. *Breast Cancer (Dove Med Press)* 2016;**8**: 183-97.

16. Wagner JP, Wolf-Yadlin A, Sevecka M, Grenier JK, Root DE, Lauffenburger DA, MacBeath G. Receptor tyrosine kinases fall into distinct classes based on their inferred signaling networks. *Sci Signal*

2013;**6**: ra58.

17. Chong CR, Janne PA. The quest to overcome resistance to EGFR-targeted therapies in cancer. *Nat Med* 2013;**19**: 1389-400.

18. Wilson TR, Fridlyand J, Yan Y, Penuel E, Burton L, Chan E, Peng J, Lin E, Wang Y, Sosman J, Ribas A, Li J, et al. Widespread potential for growth-factor-driven resistance to anticancer kinase inhibitors. *Nature* 2012;**487**: 505-9.

19. Eide CA, Adrian LT, Tyner JW, Mac Partlin M, Anderson DJ, Wise SC, Smith BD, Petillo PA, Flynn DL, Deininger MW, O'Hare T, Druker BJ. The ABL switch control inhibitor DCC-2036 is active against the chronic myeloid leukemia mutant BCR-ABLT315I and exhibits a narrow resistance profile. *Cancer Res* 2011;**71**: 3189-95.

20. Chan WW, Wise SC, Kaufman MD, Ahn YM, Ensinger CL, Haack T, Hood MM, Jones J, Lord JW, Lu WP, Miller D, Patt WC, et al. Conformational control inhibition of the BCR-ABL1 tyrosine kinase, including the gatekeeper T315I mutant, by the switch-control inhibitor DCC-2036. *Cancer Cell* 2011;**19**: 556-68.

21. Shen Y, Shi X, Pan J. The conformational control inhibitor of tyrosine kinases DCC-2036 is effective for imatinib-resistant cells expressing T674I FIP1L1-PDGFRalpha. *PLoS One* 2013;**8**: e73059.

22. Zheng MW, Zhang CH, Chen K, Huang M, Li YP, Lin WT, Zhang RJ, Zhong L, Xiang R, Li LL, Liu XY, Wei YQ, et al. Preclinical Evaluation of a Novel Orally Available SRC/Raf/VEGFR2 Inhibitor, SKLB646, in the Treatment of Triple-Negative Breast Cancer. *Mol Cancer Ther* 2016;**15**: 366-78.

23. Leconet W, Chentouf M, du Manoir S, Chevalier C, Sirvent A, Ait-Arsa I, Busson M, Jarlier M, Radosevic-Robin N, Theillet C, Chalbos D, Pasquet JM, et al. Therapeutic Activity of Anti-AXL Antibody against Triple-Negative Breast Cancer Patient-Derived Xenografts and Metastasis. *Clin Cancer Res* 2017;**23**: 2806-16.

24. Linklater ES, Tovar EA, Essenburg CJ, Turner L, Madaj Z, Winn ME, Melnik MK, Korkaya H, Maroun CR, Christensen JG, Steensma MR, Boerner JL, et al. Targeting MET and EGFR crosstalk signaling in triple-negative breast cancers. *Oncotarget* 2016;**7**: 69903-15.

25. Jin Y, Ding K, Li H, Xue M, Shi X, Wang C, Pan J. Ponatinib efficiently kills imatinib-resistant chronic eosinophilic leukemia cells harboring gatekeeper mutant T674I FIP1L1-PDGFRalpha: roles of Mcl-1 and beta-catenin. *Mol Cancer* 2014;**13**: 17.

26. Bu Q, Cui L, Li J, Du X, Zou W, Ding K, Pan J. SAHA and S116836, a novel tyrosine kinase inhibitor, synergistically induce apoptosis in imatinib-resistant chronic myelogenous leukemia cells. *Cancer Biol Ther* 2014;**15**: 951-62.

27. Shen Y, Ren X, Ding K, Zhang Z, Wang D, Pan J. Antitumor activity of S116836, a novel tyrosine kinase inhibitor, against imatinib-resistant FIP1L1-PDGFRalpha-expressing cells. *Oncotarget* 2014;**5**: 10407-20.

28. Zhu J, Feng Y, Ke Z, Yang Z, Zhou J, Huang X, Wang L. Down-regulation of miR-183 promotes migration and invasion of osteosarcoma by targeting Ezrin. *Am J Pathol* 2012;**180**: 2440-51.

29. Montero JC, Esparis-Ogando A, Re-Louhau MF, Seoane S, Abad M, Calero R, Ocana A, Pandiella A. Active kinase profiling, genetic and pharmacological data define mTOR as an important common target in triple-negative breast cancer. *Oncogene* 2014;**33**: 148-56.

30. Zhong J, Cao RX, Liu JH, Liu YB, Wang J, Liu LP, Chen YJ, Yang J, Zhang QH, Wu Y, Ding WJ, Hong T, et al. Nuclear loss of protein arginine N-methyltransferase 2 in breast carcinoma is

associated with tumor grade and overexpression of cyclin D1 protein. *Oncogene* 2014;**33**: 5546-58.

31. Livak KJ, Schmittgen TD. Analysis of relative gene expression data using real-time quantitative PCR and the 2(-Delta Delta C(T)) Method. *Methods* 2001;**25**: 402-8.

32. Alvarado D, Ligon G, Lillquist J, Seibel S, Wallweber G, Neumeister V, Rimm D, McMahon G, LaVallee T. ErbB activation signatures as potential biomarkers for anti-ErbB3 treatment in HNSCC. *PLoS ONE* 2017;**12**: e0181356.

33. Liu W, Zhou J, Qi F, Bensdorf K, Li Z, Zhang H, Qian H, Huang W, Cai X, Cao P, Wellner A, Gust R. Synthesis and biological activities of 2-amino-thiazole-5-carboxylic acid phenylamide derivatives. *Arch Pharm (Weinheim)* 2011;**344**: 451-8.

34. Asiedu MK, Beauchamp-Perez FD, Ingle JN, Behrens MD, Radisky DC, Knutson KL. AXL induces epithelial-to-mesenchymal transition and regulates the function of breast cancer stem cells. *Oncogene* 2014;**33**: 1316-24.

35. Axelrod H, Pienta KJ. Axl as a mediator of cellular growth and survival. *Oncotarget* 2014;**5**: 8818-52.

36. Palafox M, Ferrer I, Pellegrini P, Vila S, Hernandez-Ortega S, Urruticoechea A, Climent F, Soler MT, Munoz P, Vinals F, Tometsko M, Branstetter D, et al. RANK induces epithelial-mesenchymal transition and stemness in human mammary epithelial cells and promotes tumorigenesis and metastasis. *Cancer Res* 2012;**72**: 2879-88.

37. Bernardi R, Gianni L. Hallmarks of triple negative breast cancer emerging at last? *Cell Res* 2014;**24**: 904-5.

38. Hatem R, Labiod D, Chateau-Joubert S, de Plater L, El Botty R, Vacher S, Bonin F, Servely JL, Dieras V, Bieche I, Marangoni E. Vandetanib as a potential new treatment for estrogen receptor-negative breast cancers. *Int J Cancer* 2016;**138**: 2510-21.

39. Finn RS, Bengala C, Ibrahim N, Roche H, Sparano J, Strauss LC, Fairchild J, Sy O, Goldstein LJ. Dasatinib as a single agent in triple-negative breast cancer: results of an open-label phase 2 study. *Clin Cancer Res* 2011;**17**: 6905-13.

40. Moreno-Aspitia A, Morton RF, Hillman DW, Lingle WL, Rowland KM, Jr., Wiesenfeld M, Flynn PJ, Fitch TR, Perez EA. Phase II trial of sorafenib in patients with metastatic breast cancer previously exposed to anthracyclines or taxanes: North Central Cancer Treatment Group and Mayo Clinic Trial N0336. *J Clin Oncol* 2009;**27**: 11-5.

41. Park BJ, Whichard ZL, Corey SJ. Dasatinib synergizes with both cytotoxic and signal transduction inhibitors in heterogeneous breast cancer cell lines--lessons for design of combination targeted therapy. *Cancer Lett* 2012;**320**: 104-10.

42. Wu X, Liu X, Koul S, Lee CY, Zhang Z, Halmos B. AXL kinase as a novel target for cancer therapy. *Oncotarget* 2014;**5**: 9546-63.

43. Hsu YH, Yao J, Chan LC, Wu TJ, Hsu JL, Fang YF, Wei Y, Wu Y, Huang WC, Liu CL, Chang YC, Wang MY, et al. Definition of PKC-alpha, CDK6, and MET as therapeutic targets in triple-negative breast cancer. *Cancer Res* 2014;**74**: 4822-35.

44. Mazzone M, Comoglio P. The Met pathway: master switch and drug target in cancer progression. *FASEB J* 2006;**20**: 1611-21.

45. Eckert M, Lwin T, Chang A, Kim J, Danis E, Ohno-Machado L, Yang J. Twist1-induced invadopodia formation promotes tumor metastasis. *Cancer Cell* 2011;**19**: 372-86.

46. Ivaska J. Vimentin: Central hub in EMT induction? *Small GTPases* 2011;**2**: 51-3.

47. Vuoriluoto K, Haugen H, Kiviluoto S, Mpindi J, Nevo J, Gjerdrum C, Tiron C, Lorens J,

Ivaska J. Vimentin regulates EMT induction by Slug and oncogenic H-Ras and migration by governing Axl expression in breast cancer. *Oncogene* 2011;**30**: 1436-48.

48. Asiedu M, Beauchamp-Perez F, Ingle J, Behrens M, Radisky D, Knutson K. AXL induces epithelial-to-mesenchymal transition and regulates the function of breast cancer stem cells. *Oncogene* 2014;**33**: 1316-24.

49. Leconet W, Chentouf M, du Manoir S, Chevalier C, Sirvent A, Aït-Arsa I, Busson M, Jarlier M, Radosevic-Robin N, Theillet C, Chalbos D, Pasquet J, et al. Therapeutic Activity of Anti-AXL Antibody against Triple-Negative Breast Cancer Patient-Derived Xenografts and Metastasis. *Clin Cancer Res* 2017;**23**: 2806-16.

50. D'Alfonso T, Hannah J, Chen Z, Liu Y, Zhou P, Shin S. Axl receptor tyrosine kinase expression in breast cancer. *J Clin Pathol* 2014;**67**: 690-6.

51. Carey LA, Rugo HS, Marcom PK, Mayer EL, Esteva FJ, Ma CX, Liu MC, Storniolo AM, Rimawi MF, Forero-Torres A, Wolff AC, Hobday TJ, et al. TBCRC 001: randomized phase II study of cetuximab in combination with carboplatin in stage IV triple-negative breast cancer. *J Clin Oncol* 2012;**30**: 2615-23.

52. Hong J, Peng D, Chen Z, Sehdev V, Belkhiri A. ABL regulation by AXL promotes cisplatin resistance in esophageal cancer. *Cancer Res* 2013;**73**: 331-40.

53. Rankin EB, Fuh KC, Taylor TE, Krieg AJ, Musser M, Yuan J, Wei K, Kuo CJ, Longacre TA, Giaccia AJ. AXL is an essential factor and therapeutic target for metastatic ovarian cancer. *Cancer Res* 2010;**70**: 7570-9.

54. Hong CC, Lay JD, Huang JS, Cheng AL, Tang JL, Lin MT, Lai GM, Chuang SE. Receptor tyrosine kinase AXL is induced by chemotherapy drugs and overexpression of AXL confers drug resistance in acute myeloid leukemia. *Cancer Lett* 2008;**268**: 314-24.

55. Chisholm C, Wang H, Wong A, Vazquez-Ortiz G, Chen W, Xu X, Deng C. Ammonium tetrathiomolybdate treatment targets the copper transporter ATP7A and enhances sensitivity of breast cancer to cisplatin. *Oncotarget* 2016;**7**: 84439-52.

Figure legends

Figure 1. DCC-2036 significantly inhibits human TNBC cell proliferation. **A,** MDA-MB-231, HS-578T (TNBC cells) and MCF-7 cells (luminal cells, positive control) were exposed to increased concentrations of DCC-2036 for 72 h followed by the MTS assay. The data are from experiments performed in triplicate and are expressed as the mean±standard deviation (SD). **B,** Clonogenicity of TNBC cells is inhibited by DCC-2036. TNBC cells were treated with 3.75 μM DCC-2036 for 48 h and then harvested, washed, and plated in drug-free DMEM. After 14 days, the number of colonies was counted. Left, representative graphs of three independent experiments; right, statistical charts. Columns, mean; bars, SD. Student's *t* test. ***P<0.0001. **C,** DCC-2036 induces G1 arrest in TNBC cells. TNBC cells were cultured with 3.75 μM DCC-2036 for 48 h, and cells were then collected, washed, fixed, stained with propidium iodide and analyzed with flow cytometry. Left, representative graphs of three independent experiments; right, statistical charts. Columns, mean; error bars, SD. Student's *t* test, **P<0.01, *** *P*<0.0001.

Figure 2. DCC-2036 induces apoptosis and inhibits migration and invasion of human TNBC cells. **A,** MDA-MB-231 cells, HS-578T cells (TNBC cells) and MCF-7 cells (positive control) were cultured with DCC-2036 at the indicated concentrations for 48 h, and cells were then collected, washed and stained with Annexin V-FITC/PI to detect the cell apoptosis with flow cytometry. Top, representative of three independent experiments; bottom, statistical charts with vertical axis representing the sum of all dead cells, except the left lower quadrant. One-way ANOVA with *post hoc* compared with control by Tukey's test. **P<0.01, ***P<0.0001. The data are expressed as the mean±SD. **B,** Transwell assay of human TNBC cells treated with 3.75 μM DCC-2036 for 48 h. Left, representative images of migratory and invasive cells on polycarbonate Transwell membrane, 10×; right, the percentage of migratory and invasive cells from three independent experiments is shown. Columns, mean; error bars, SD. Student's *t* test, ***P<0.0001.

Figure 3. DCC-2036 inhibits the PI3K/Akt-NFκβ pathway and epithelial-mesenchymal transition (EMT) by targeting AXL/MET in TNBC cells. **A,** DCC-2036 reduces AXL and MET mRNA levels significantly in TNBC cells. MDA-MB-231 cells were treated with 3.75 μM DCC-2036 for 48 h, and the mRNA levels of AXL and MET were analyzed by real-time PCR. Columns, mean; error bars, SD. Student's t test, ***P<0.0001. **B,** DCC-2036 impacts the phosphorylated and total levels of AXL and MET in different subtypes of breast cancer cell lines. MDA-MB-231, HS-578T (TNBC cells) and MCF-7 cells (positive control) were exposed to indicated concentrations of DCC-2036 for 48 h, and the phosphorylated and total levels of AXL and MET were analyzed by immunoblotting. **C,** Overexpression of AXL or MET attenuates DCC-2036-induced apoptosis in MDA-MB-231 cells. MDA-MB-231 cells were transfected with human AXL plasmid, human MET plasmid or vector plasmid. Cells were then exposed to 5 μM DCC-2036 for 48 h. Levels of indicated proteins were analyzed by immunoblotting (upper). Cell death was detected with trypan blue in triplicate (lower). Columns, mean; error bars, SD. Student's t test, *P<0.05, **P<0.01. **D,** DCC-2036 downregulates the PI3K/Akt-NFκβ pathway in TNBC cells. Immunoblot analyses of P-Akt, P-IκBα, P-p65 expression and their total protein levels in MDA-MB-231 cells and HS-578T cells treated with indicated concentrations of DCC-2036 for 48 h. Actin bands for MDA-MB-231 and HS-578T are identical with Fig. 3B and from the same experimental setup. **E,** DCC-2036 inhibits degradation of IκBα and relocation of p65. MDA-MB-231 cells were incubated with 3.75 μM DCC-2036 for 48 h. Cytoplasmic (left) and nuclear (right) extracts were then examined by immunoblotting. Actin and Lamin B served as markers of cytoplasmic and nuclear extracts, respectively. **F,** DCC-2036 regulates the expression of EMT markers in TNBC cells. MDA-MB-231 and HS-578T cells were treated with DCC-2036 at the indicated concentrations for 48 h, and levels of EMT-related proteins then detected by Western blotting.

Figure 4. DCC-2036 attenuates the growth and metastasis of xenografted MDA-MB-231 tumors transplanted in NSG mice. **A,** Growth curves of subcutaneous

xenografts of MDA-MB-231 cells. NSG mice bearing MDA-MB-231 xenograft tumors were treated with control (0.5% carboxymethylcellulose/1% Tween 80) or DCC-2036 (100 mg/kg/d, oral gavage administration) for 22 d. The estimated tumor volume was plotted versus time. Points, mean; bars, SD. **B,** The body weight change of mice after treatment with DCC-2036. **C,** Weights of tumors dissected on day 22 post-treatment: columns, mean; bars, SD. Student's *t* test (lower). Images of representative tumors are shown (upper). **D,** Metastasis incidence in the lungs of mice after treatment with DCC-2036 (upper). Representative images of H&E staining from control and DCC-2036 treatment groups (lower, 40×). **E,** Immunohistochemical analysis using Ki67 as well as H&E staining in xenograft tissues from mice (40×). Scale bars, 20 μm. **F,** Immunoblotting of xenograft tissues from mice on day 22 post-treatment.

Figure 5. Effect of DCC-2036 in NSG mice with basal-like TNBC patient-tumor xenografts (PDX). **A,** mRNA and protein levels of AXL and MET in two basal-like TNBC PDXs, IDMO-129 and 862812, based on real-time PCR and Western blot analysis. Columns, mean; error bars, SD. Student's *t* test, ***$P<0.0001$. **B,** Growth curves of subcutaneous xenografts of IDMO-129 and 862812. Mice engrafted with the AXL/MET-high PDX IDMO-129 and AXL/MET-low PDX 862812 were left untreated or treated with 150 mg/kg DCC-2036 once daily. The results are presented as the mean±SEM in each group (n=7). Student's *t* test, *$P<0.05$. **C,** Body weight change of mice after treatment with DCC-2036 in IDMO-129 and 862812. **D,** Weights of tumors dissected at the end of experiments (day 63 post-treatment) in IDMO-129 PDX: columns, mean; bars, SEM. Student's *t* test, *$P<0.05$ (lower). Images of representative tumors are shown (upper). **E,** Weights of tumors dissected at the end of experiments (day 53 post-treatment) in 862812 PDX: columns, mean; bars, SEM (lower). Images of representative tumors are shown (upper). **F,** Immunohistochemical analysis using AXL, MET and Ki67 as well as H&E staining in xenograft tissues from IDMO-129 PDX (40×). Scale bars, 20 μm. **G,** Immunoblot of xenograft tissues from IDMO-129 PDX on day 63 post-treatment.
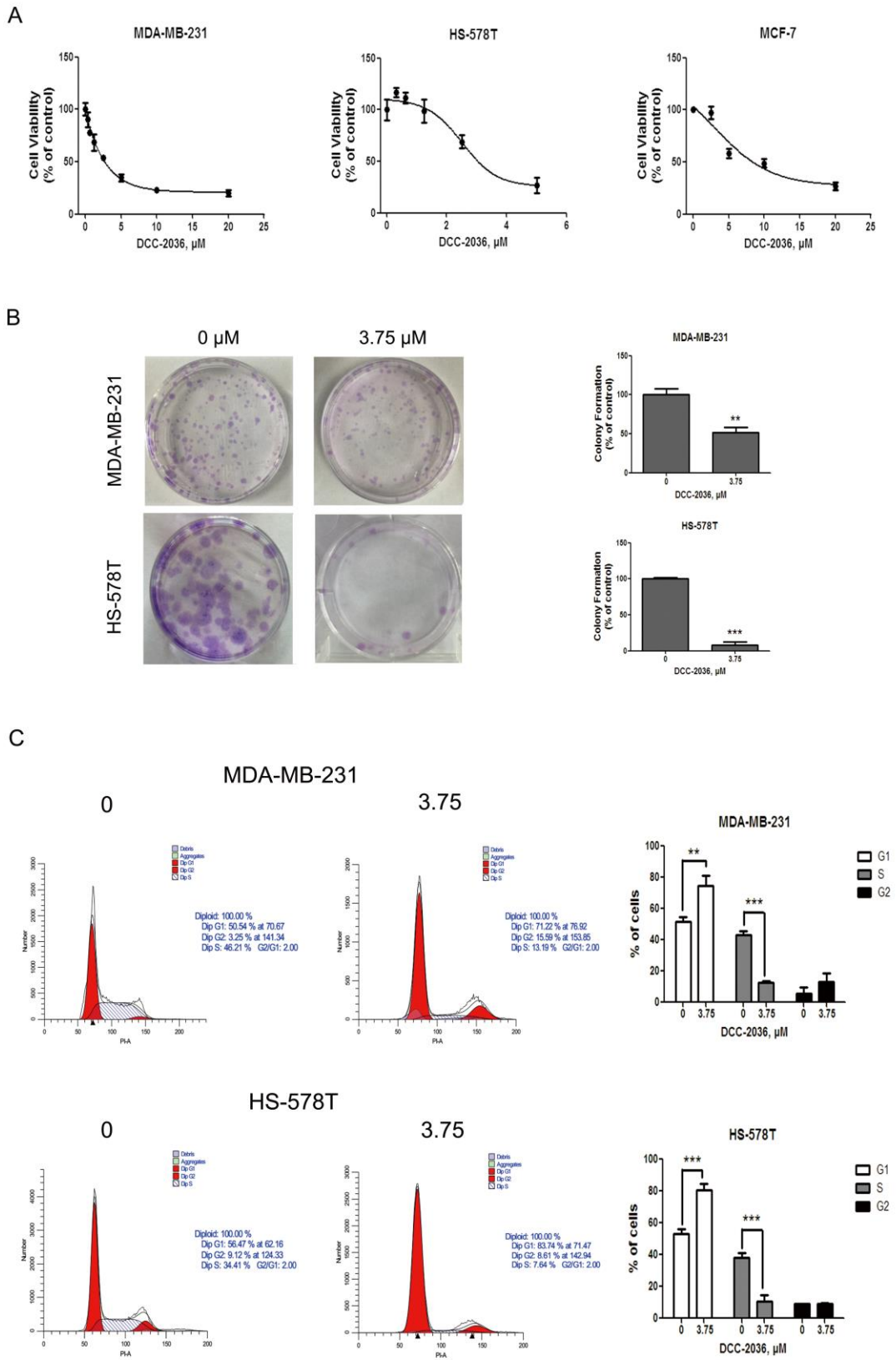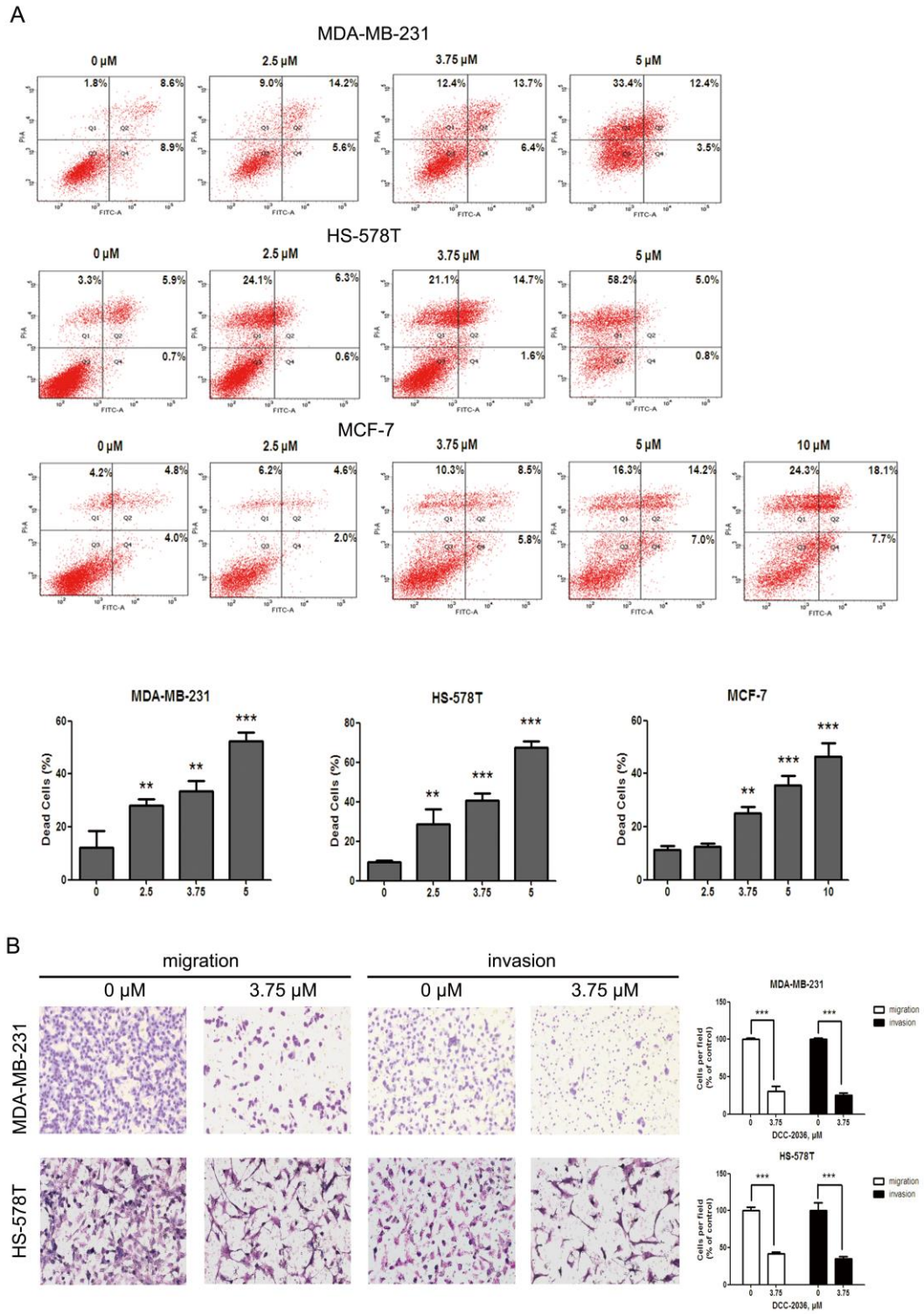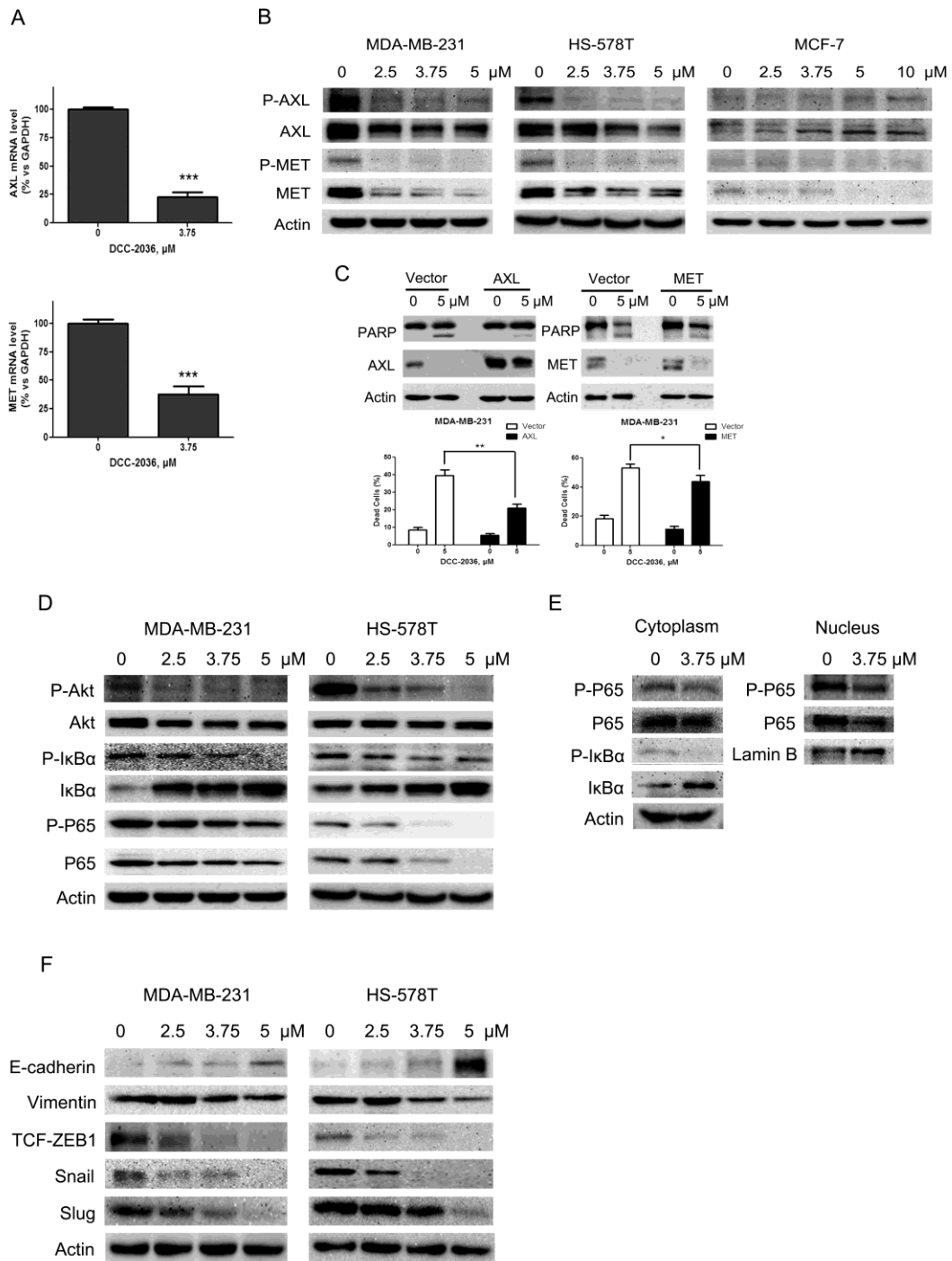
Figure 1
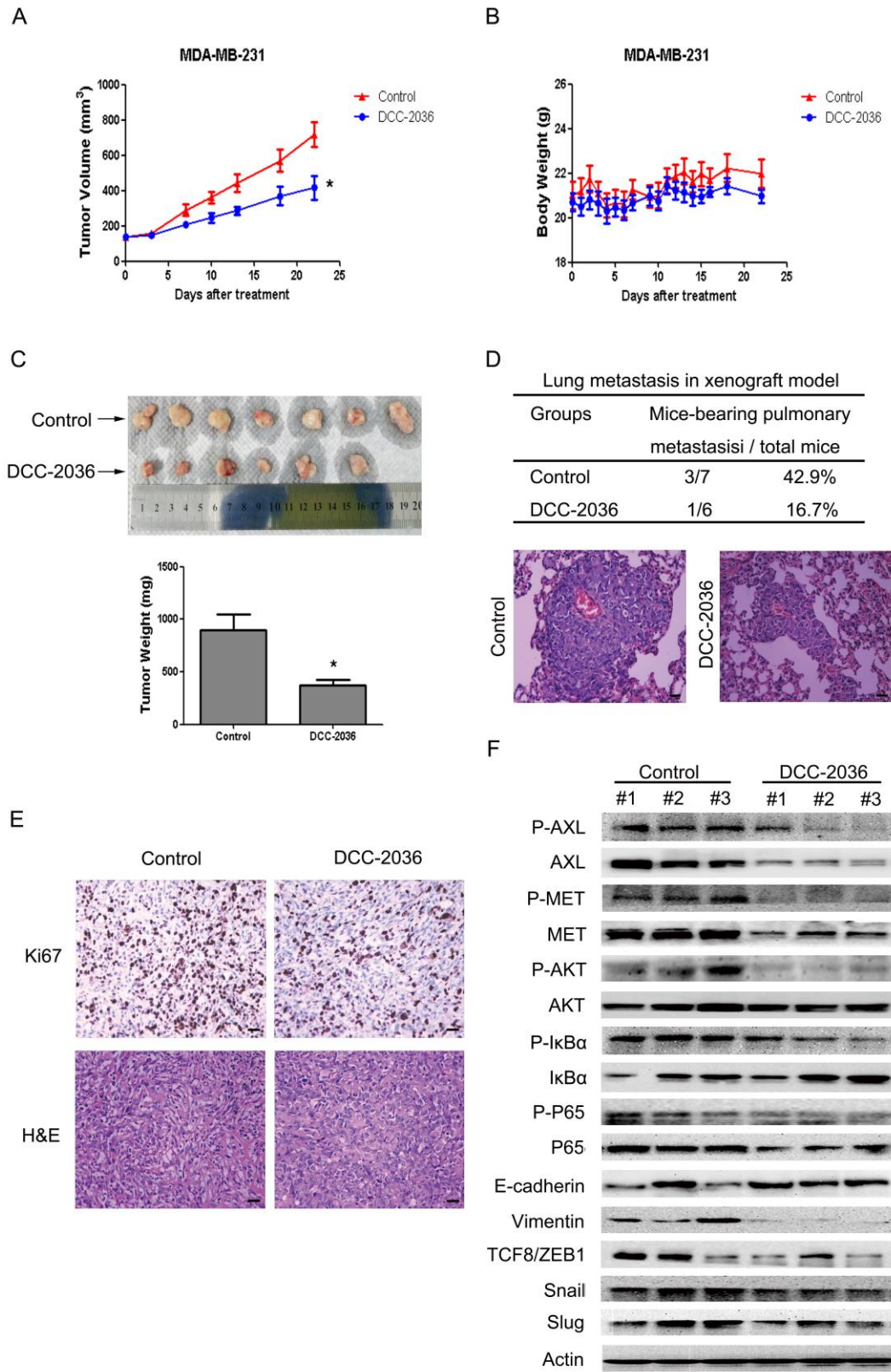
A

B

C

Figure 2

A

B

Figure 3

Figure 4

A
MDA-MB-231

B
MDA-MB-231

C

Control →

DCC-2036 →

D
Lung metastasis in xenograft model

Groups	Mice-bearing pulmonary metastasisi / total mice	
Control	3/7	42.9%
DCC-2036	1/6	16.7%

Control   DCC-2036

E
          Control   DCC-2036

Ki67

H&E

F

          Control   DCC-2036
          #1   #2   #3   #1   #2   #3

P-AXL
AXL
P-MET
MET
P-AKT
AKT
P-IκBα
IκBα
P-P65
P65
E-cadherin
Vimentin
TCF8/ZEB1
Snail
Slug
Actin

Figure 5
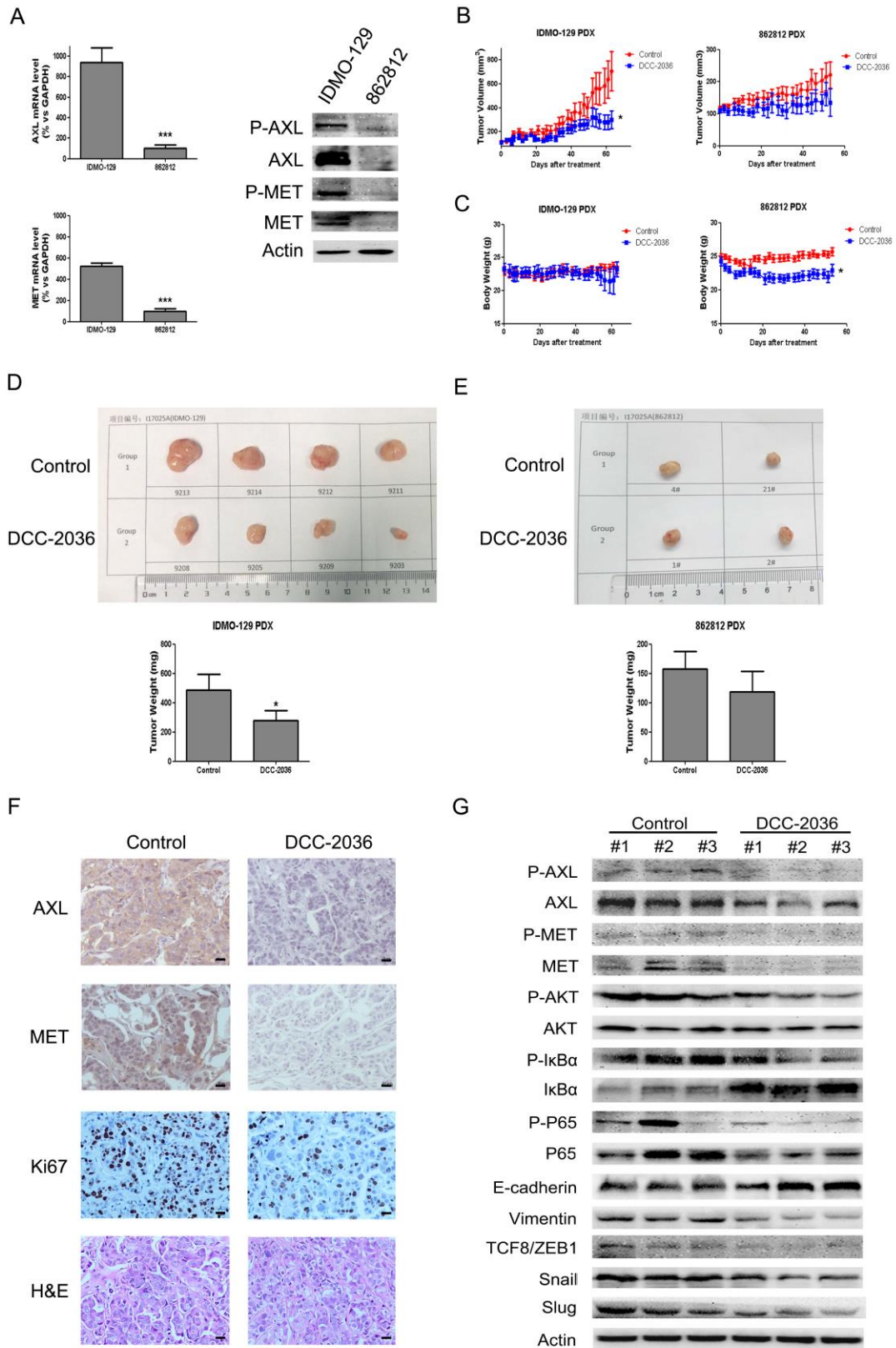
Table 1. Antiproliferative effects against MDA-MB-231 and HS-578T human TNBC cell lines.

Compound	IC$_{50}$, [μM][a,b]	
	MDA-MB-231	HS-578T
DCC-2036	3.3	3.7
cisplatin	21.9	7.2
Paclitaxel	0.017	0.036
gemcitabine	>40	>40
Doxorubicin	0.01	0.15
lapatinib	12.8	6.6
tamoxifen (TAM)	18.9	11.2
5-FU	9.6[c]	
Gefitinib	7.3[c]	

[a]The IC$_{50}$ values represent the concentration which results in a 50% decrease in cell growth after 72 h incubation. [b]Values are the means of at least 3 experiments. [c]Data cited from *ref.33*.

Triple-negative breast cancer (TNBC) is not sensitive to hormonal therapies or treatments targeted against HER2. Tyrosine kinases (TKs) could be potential targets due to their activation and high expression in multiple TNBC subtypes. This study shows that DCC-2036, a third-generation tyrosine kinase inhibitor with high selective activity for multiple TKs, has potent activity against TNBC. DCC-2036 targets AXL/MET and regulates the downstream PI3K/Akt-NFκβ pathway in vitro and in vivo, without apparent toxicity. Moreover, DCC-2036 exhibits more efficient anti-proliferative activity than most clinical drugs. These data highlight DCC-2036 as a promising targeting agent for treating TNBC, especially tumors that overexpress AXL/MET.